



Advancing CO₂ conversion: integrated use of dual active catalytic sites in flexible, porous polymeric porphyrin and ionic liquid composite networks

Liping Zheng¹, Can Fang¹, Zhenghai Chen², Jingxu Han¹, Zhouxian Wang¹, Tonghao Dai¹, Jiacong Ma¹, Zhifeng Dai^{1,3,*} , Yubing Xiong^{1,3,*} , Qi Sun^{4,*}

Keywords:

Porous organic polymer, porphyrin, ionic liquid, CO₂ transformation, synergistic catalysis

Citation:

Zheng, L.; Fang, C.; Chen, Z.; Han, J.; Wang, Z.; Dai, T.; Ma, J.; Dai, Z.; Xiong, Y.; Sun, Q. Advancing CO₂ conversion: integrated use of dual active catalytic sites in flexible, porous polymeric porphyrin and ionic liquid composite networks. *Chem. Synth.* 2026, 6, 12. <https://dx.doi.org/10.20517/cs.2024.92>

Received: 30 Jul 2024

First Decision: 25 Nov 2024

Revised: 16 Dec 2024

Accepted: 23 Dec 2024

Published: 26 Jan 2026

Academic Editor:

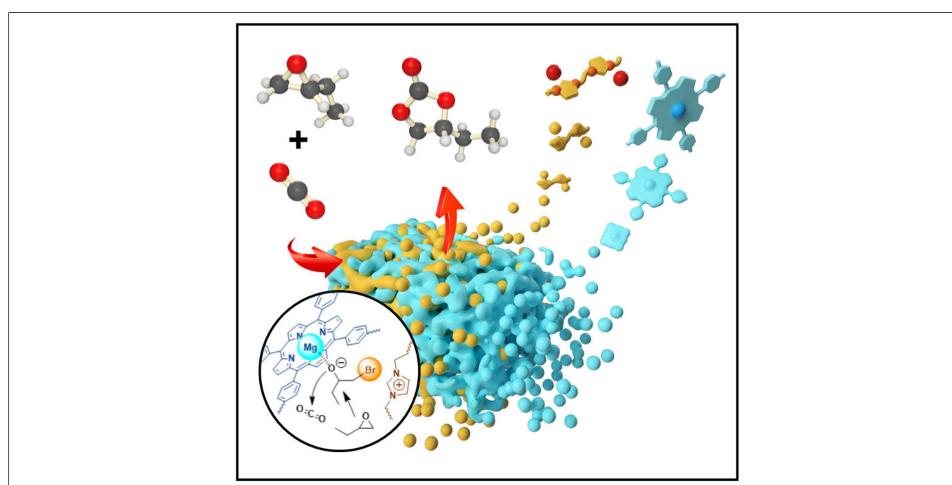
Da-Gang Yu

Copy Editor:

Pei-Yun Wang

Production Editor:

Pei-Yun Wang



Abstract

The development of highly efficient, multifunctional catalysts featuring cooperative active sites is a complex yet vital endeavor. This study introduces an innovative approach through *in situ* polymerization, where flexible, cross-linked ionic polymers are synthesized within the channels of flexible, porous polymeric porphyrins. This process yields a series of interwoven frameworks endowed with dual catalytic active sites. The uniqueness of these catalysts lies in the synergistic interaction between metalated porphyrins and ionic components, greatly boosting their catalytic efficiency in the cycloaddition of CO₂ and epoxides. The bifunctional catalysts not only surpass the individual constituents in performance but also demonstrate a significant superiority over their physical mixture. The structural flexibility and high density of active sites in these catalysts enable synergistic effects, leading to exceptional catalytic performance. This research marks a substantial leap in catalyst design, introducing a novel method for crafting bifunctional catalysts with dual-activation capabilities.

¹Key Laboratory of Surface & Interface Science of Polymer Materials of Zhejiang Province, School of Chemistry and Chemical Engineering, Zhejiang Sci-Tech University, Hangzhou 310018, Zhejiang, China.

²Kente Catalysts Inc., Taizhou 317306, Zhejiang, China.

³Zhejiang Sci-Tech University, Shengzhou Innovation Research Institute, Shengzhou 312400, Zhejiang, China.

⁴Zhejiang Provincial Key Laboratory of Advanced Chemical Engineering Manufacture Technology, College of Chemical and Biological Engineering, Zhejiang University, Hangzhou, 310027, Zhejiang, China.

*Correspondence to: Prof. Qi Sun, Zhejiang Provincial Key Laboratory of Advanced Chemical Engineering Manufacture Technology, College of Chemical and Biological Engineering, Zhejiang University, Hangzhou 310027, Zhejiang, China. E-mail: sunqichs@zju.edu.cn; Prof. Yubing Xiong, Dr. Zhifeng Dai, Key Laboratory of Surface & Interface Science of Polymer Materials of Zhejiang Province, School of Chemistry and Chemical Engineering, Zhejiang Sci-Tech University, Hangzhou 310018, Zhejiang, China. E-mail: yubing_xiong@163.com; daizhifeng1988@163.com

INTRODUCTION

The escalating levels of CO₂ in the atmosphere present significant global environmental challenges^[1-4]. Tackling the increasing accumulation of CO₂ is a critical issue, particularly focusing on its capture and conversion into useful substances^[5-15]. Interestingly, CO₂ offers several advantages as a resource: it is abundant, non-toxic, inexpensive, and renewable, making it an ideal C1 source for creating valuable organic compounds^[16-19]. Hence, converting CO₂ into value-added products is not only crucial for industrial processes but also a significant area of academic research, aiding in carbon recycling efforts.

One effective method for utilizing CO₂ is through its cycloaddition with epoxides to produce cyclic carbonates, which are extensively used in various industries^[20-35]. Numerous catalytic systems have been investigated for this transformation, with the dual catalytic system combining Lewis acid and organic ionic molecular catalysts emerging as a particularly effective approach, allowing the reaction to occur under atmospheric conditions^[36-43]. In the quest for complete recyclability of catalytic components, attention has shifted to heterogeneous bifunctional catalytic systems. These systems seek to address the spatial separation issue observed in traditional supported catalysts, a factor that frequently impedes efficient catalysis. The proposed strategy involves integrating halogen anion-containing flexible linear polymers with rigid frameworks such as covalent organic frameworks (COFs) or metal-organic frameworks (MOFs), which have Lewis acid centers^[44-46]. This combination is designed to foster a synergistic interaction between the two types of catalytic centers. However, a notable challenge in this approach is the potential loss of the linear polymers from the framework materials during extended reactions, due to the absence of specific interactions between these components. Addressing this issue is crucial for the long-term stability and efficiency of the catalytic system.

Recent studies have highlighted that polymers created through vinyl free-radical polymerization exhibit remarkable flexibility in solvent environments, enabling synergistic interactions between the functional species on the polymer chains^[47-56]. Building on this insight, we investigated the use of polymers derived from vinyl polymerization that incorporate Lewis acid functionalities. These polymers were paired with cross-linked polyionic liquids to develop bifunctional synergistic catalysts. This innovative pairing of two flexible frameworks not only facilitates interactions between different active sites but also significantly improves the overall stability of the catalyst. For this approach, we utilized a porous organic polymer (POP), synthesized from a Mg metalated, vinyl-functionalized tetraphenylporphyrin monomer (v-TPPMg), as the primary host material [polymeric v-TPPMg (POP-TPPMg)]. Into this framework, we introduced the monomer 3,3'-(ethane-1,2-diyl)bis(1-vinyl-1H-imidazol-3-ium) bromide (v-BIL), infusing it into the pore channels of POP-TPPMg. This was followed by an *in-situ* polymerization process, resulting in a distinctive interwoven framework structure (POP-TPPMg-BIL-x, where x represents the mole ratio of the v-BIL to v-TPPMg). The inherent flexibility of these frameworks enables a cooperative mechanism between two distinct catalytic species [Figure 1]. Moreover, the enrichment and strategic positioning of these catalytic species within the framework result in a catalytic efficiency that surpasses that of the individual constituents and their physical mixture. Importantly, this method exhibited no leaching of catalytic components, a crucial factor for the sustainable and long-term application of such catalysts in industrial processes. This novel approach not only enhances the efficiency of catalysis but also contributes significantly to the field of sustainable chemistry, addressing the urgent need to effectively utilize and transform CO₂ into valuable products.

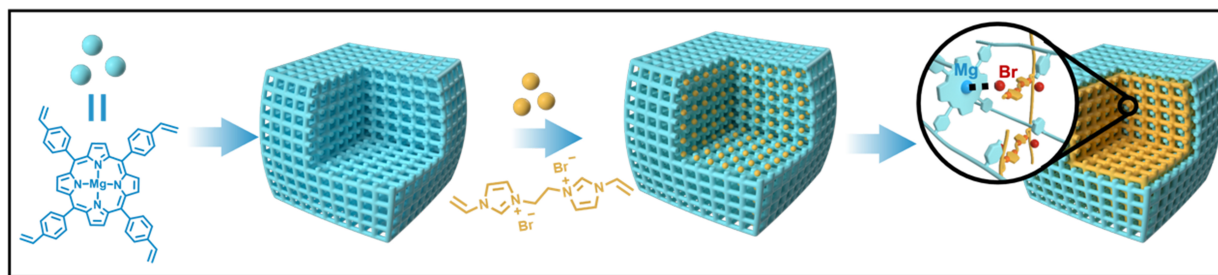


Figure 1. Conceptual schematic illustrating the creation of interwoven frameworks featuring dual catalytic active sites. The process involves the polymerization of a vinyl-functionalized Mg metalated tetraphenylporphyrin monomer acting as a Lewis acid, resulting in a porous framework. This is followed by the infiltration of a bivinyl-functionalized imidazolium salt and subsequent *in situ* polymerization to generate Lewis acid sites and Br ions within the structure.

EXPERIMENTAL

Materials

Pyrrole was obtained from Aladdin, while 4-bromostyrene was procured from Meryer Chemical Technology (Shanghai). Prior to use, both substances underwent distillation. Solvents such as tetrahydrofuran (THF) were distilled over LiAlH₄; N,N-dimethylformamide (DMF) underwent distillation over CaH₂, and dichloromethane and triethylamine were similarly distilled. Various commercially available reagents including azobisisobutyronitrile (AIBN), MgBr₂·Et₂O, 1,2-epoxybutane, 1,2-epoxyhexane, styrene oxide, allyl glycidyl ether, butyl glycidyl ether, phenyl glycidyl ether, 2-ethylhexyl glycidyl ether and cyclohexene oxide, 1-vinylimidazole, 1,2-dibromoethane, and methanol were purchased at high purity levels and utilized without further purification. These reagents are all obtained from the Shanghai Titan Scientific Co., Ltd.

Synthesis of v-BIL

The synthesis of v-BIL was carried out under a N₂ atmosphere. In a 25 mL Schlenk tube, 5 mL of methanol, 2 g (21.3 mmol) of 1-vinylimidazole, and 1.6 g (8.5 mmol) of 1,2-dibromoethane were combined and heated at 70 °C for 48 h. Upon completion of the reaction, the solvent was evaporated using a rotary evaporator, and the resulting liquid was dispersed in a small amount of methanol. This solution was then added drop by drop to 400 mL of vigorously stirred diethyl ether. The product was obtained after washing with diethyl ether and subsequently dried under vacuum overnight, yielding 3.01 g (74.9%). ¹H nuclear magnetic resonance (NMR) (400 MHz, DMSO-d₆): δ = 9.60 (m, 2H), 8.27 (t, 2H), 7.88 (d, 2H), 7.36 (dd, 2H), 5.99 (d, 2H), 5.46 (d, 2H), 4.82 (s, 4H) ppm. ¹³C NMR (400 MHz, CDCl₃): δ = 136.14, 128.86, 123.31, 109.12, 48.47 ppm.

Synthesis of 4-vinylbenzaldehyde

The synthesis of 4-vinylbenzaldehyde commenced with the addition of 4-bromostyrene (18.2 g, 100 mmol) dropwise to a THF solution containing activated magnesium at 0 °C under a N₂ atmosphere to form (4-vinylphenyl)magnesium bromide. Subsequently, an excess of DMF was added dropwise to the solution. The resulting mixture was stirred overnight at room temperature and then quenched with 50 mL of saturated NH₄Cl solution. Following extraction with ethyl acetate, washing with brine, and drying with anhydrous MgSO₄, the solution was filtered and further purified through flash column chromatography on silica gel, yielding 4-vinylbenzaldehyde (12.1 g) with a 91.7% yield. ¹H NMR (400 MHz, CDCl₃): δ = 9.99 (s, 1H), 7.84 (m, 2H), 7.55 (m, 2H), 6.77 (dd, 1H), 5.91 (d, 1H), 5.44 (d, 1H) ppm.

Synthesis of vinyl-functionalized porphyrin monomers

The synthesis of vinyl-functionalized porphyrin monomers (v-TPP) was carried out in a typical “one-pot” reaction, following a previously reported literature procedure^[36]. In a flask, pyrrole (3.45 g, 10 mmol) and 4-vinylbenzaldehyde (6.80 g, 51.5 mmol) were combined with propionic acid (250 mL) pre-heated to 140 °C.

After 1 h of reaction, the solution was cooled to room temperature. Subsequent to filtration, washing with methanol and ethyl acetate, and drying of the title compound, a purple crystalline porphyrin monomer was obtained (2.05 g) with a yield of 22.1%. ^1H NMR (400 MHz, CDCl_3): δ = 8.88 (s, 8H), 8.18 (d, 8H), 7.80 (d, 8H), 7.06 (dd, 4H), 6.07 (d, 4H), 5.50 (d, 4H), -2.73 (s, 2H) ppm.

Synthesis of v-TPPMg

The synthesis of v-TPPMg involved adding v-TPP (1.0 g, 1.4 mmol) to a three-neck round-bottom flask containing 150 mL of CH_2Cl_2 . Subsequently, 22.6 mL of triethylamine and $\text{MgBr}_2 \cdot \text{Et}_2\text{O}$ (7.16 g, 27.7 mmol) were introduced. After being stirred at room temperature for 15 min, the mixture was washed with water, the solvent was removed under vacuum, and the product was dried, yielding 0.95 g (92.0% yield). ^1H NMR (400 MHz, CDCl_3): δ = 8.89 (s, 8H), 8.19 (d, 8H), 7.79 (d, 8H), 7.07 (dd, 4H), 6.07 (d, 4H), 5.47 (d, 4H) ppm. ^{13}C NMR (400 MHz, CDCl_3): δ = 141.81, 137.06, 136.83, 134.95, 124.74, 114.79 ppm.

Synthesis of POP-TPPMg

The POP-TPPMg was synthesized through a solvothermal polymerization process using the v-TPPMg monomer. In this procedure, 1 g of v-TPPMg (equivalent to 1.3 mmol) was dissolved in 10 mL of DMF. Simultaneously, 100 mg of AIBN was added. The resulting mixture was placed in an autoclave and subjected to solvothermal conditions at 100 °C for 24 h. Following the polymerization reaction, the obtained polymer was subjected to purification steps. First, it was washed with DMF, and subsequently, a Soxhlet extractor was employed using dichloromethane (CH_2Cl_2) as the solvent for a duration of 72 h. The final product, the POP-TPPMg, was isolated with a yield of 96.0%.

Synthesis of POP-TPPMg-BIL-x

As a typical sample, POP-TPPMg-BIL-1.57 (1.57 representing the molar ratio of v-BIL to v-TPPMg) involved the dispersion of 0.2 g of POP-TPPMg in 10 mL of methanol within a 50 mL Schlenk tube. After stirring for 10 min, a mixture containing v-BIL at a quantity of 0.5 g (equivalent to 1.3 mmol) and 50 mg of AIBN was added to the solution. The resulting mixture underwent further stirring at room temperature for a duration of 24 h, following which the stirring was halted. Subsequently, the reaction system was heated to 100 °C and maintained at this temperature for an additional 24 h. After completion of the reaction, the mixture was subjected to filtration, and the obtained product was washed and dried. For other composites, the procedures are similar, except that the quantity of v-BIL varies.

Synthesis of POP-Bpy

In a typical run, 5,5'-divinyl-2,2'-bipyridine (1 g) was dissolved in DMF (10 mL), to which AIBN (25 mg) was then added. The mixture was stirred at room temperature for 3 h before being transferred to an autoclave and heated at 100 °C for 24 h. Following the reaction, DMF was extracted with ethanol, and the resulting material was dried under vacuum to yield a light yellow solid, obtained in nearly quantitative yield.

Synthesis of POP-Bpy-BIL-x (where x represents the mole ratio of Bpy to imidazole moieties)

As a typical run, 0.2 g of POP-Bpy was dispersed in 10 mL of methanol and stirred for 10 min. A solution containing 0.57 g (1.6 mmol) of v-BIL and 50 mg of AIBN was then added. The mixture was stirred at room temperature for 24 h, followed by heating at 100 °C for an additional 24 h. After the reaction was complete, the mixture was filtered, and the resulting product was washed with methanol and dried. The final product was designated as POP-Bpy-BIL-0.86, indicating the mole ratio of Bpy to imidazole moieties. The synthesis of POP-Bpy-BIL-0.14 followed the same procedure as for POP-Bpy-BIL-0.86, but started with 0.2 g of POP-Bpy and 0.13 g of v-BIL.

Synthesis of POP-BpyCu-BIL-x

To synthesize POP-BpyCu-BIL-x, 250 mg of either POP-Bpy-BIL-0.86 or POP-Bpy-BIL-0.14 was swollen in 10 mL of DMF. Subsequently, 16.5 mg of $\text{Cu}(\text{OAc})_2 \cdot \text{H}_2\text{O}$ was added to the solution. The mixture was stirred at room temperature for 12 h. After stirring, the product was collected by filtration, sequentially washed with excess DMF, ethanol, and acetone, and then dried at 60 °C under vacuum. The synthesized products were designated as POP-BpyCu-BIL-0.86 and POP-BpyCu-BIL-0.14, with their copper contents determined to be 2.38 wt% and 2.69 wt%, respectively, as measured by inductively coupled plasma-optical emission spectrometry (ICP-OES).

Synthesis of polymeric v-BIL

Polymeric v-BIL (PBIL) was synthesized through the free radical polymerization of the v-BIL monomer. In a typical procedure, 1 g of v-BIL and 50 mg of AIBN were dissolved in 10 mL of MeOH and transferred to an autoclave for 24 h at 100 °C. Following the polymerization, the resulting polymer was washed with CH_2Cl_2 and dried under vacuum for 10 h at 60 °C, yielding the PBIL catalyst (0.95 g, 95.0% yield).

Characterization

^1H NMR spectra were acquired using a Bruker Avance-400 (400 MHz) spectrometer (Bruker, Germany). Chemical shifts were reported in parts per million (ppm) relative to tetramethylsilane (TMS) at $\delta = 0$ ppm. Solid-state cross-polarization magic angle spinning ^{13}C (MAS) NMR spectra were recorded on a Varian infinity plus 400 M spectrometer (Varian, American), equipped with a magic-angle spin probe, in a 4-mm ZrO_2 rotor. N_2 sorption isotherms, collected at -196 °C, were measured using a Micromeritics ASAP 2020M system (Micromeritics, American), and the samples were pre-treated under vacuum at 100 °C for 12 h. Surface areas were calculated employing the Brunauer–Emmett–Teller (BET) method. Thermal gravimetric analysis (TGA) experiments were conducted on a SDT Q600 V8.2 Build100 thermogravimetric analyzer under a N_2 flow. CO_2 sorption isotherms were obtained at 25 and 0 °C under 1 atm CO_2 pressure using Micromeritics ASAP2010. Prior to measurement, the samples underwent vacuum treatment at 100 °C for 12 h. X-ray photoelectron spectroscopy (XPS) spectra were recorded on a Thermo ESCALAB 250 (Thermo, American) with Al $\text{K}\alpha$ irradiation at $\theta = 90^\circ$ for X-ray sources. Binding energies were calibrated using the C1s peak at 284.9 eV. Elemental analysis was conducted using the Vario micro cube Organic Element Analyzer (Elementar, Germany). Scanning electron microscopy (SEM) images were captured using a Hitachi SU 8000 apparatus. Transmission electron microscopy (TEM) experiments were conducted on a JEM-2100F field emission electron microscope (JEOL, Japan) with an acceleration voltage of 110 kV. The metal content in the catalysts was quantified by ICP-OES (Agilent 730).

Catalytic cycloaddition of epoxides with CO_2

The catalytic cycloaddition reactions were conducted in a 25 mL Schlenk tube containing a specific quantity of epoxides and diverse catalysts. The system underwent three vacuum purges, followed by the introduction of CO_2 via a balloon. The transformation of epoxide was tracked using ^1H NMR spectroscopy. In recycling trials, the catalyst was isolated through centrifugation, washed with CH_2Cl_2 three times, and dried under vacuum before its application in successive runs.

RESULTS AND DISCUSSION

Catalyst characterization

The formation of the interwoven framework structures in this study was achieved by integrating v-BIL monomers into the pore channels of the POP-TPPMg. This polymer was initially synthesized through the free radical-induced polymerization of vinyl groups, followed by the *in-situ* polymerization of the v-BIL monomers [Supplementary Figures 1 and 2]. The resulting composite materials were designated as POP-TPPMg-BIL-x. Experimental evaluations revealed that these composites are insoluble in common solvents such as DMF and CHCl_3 . Thermal gravity (TG) analysis further indicated the thermal stability of the

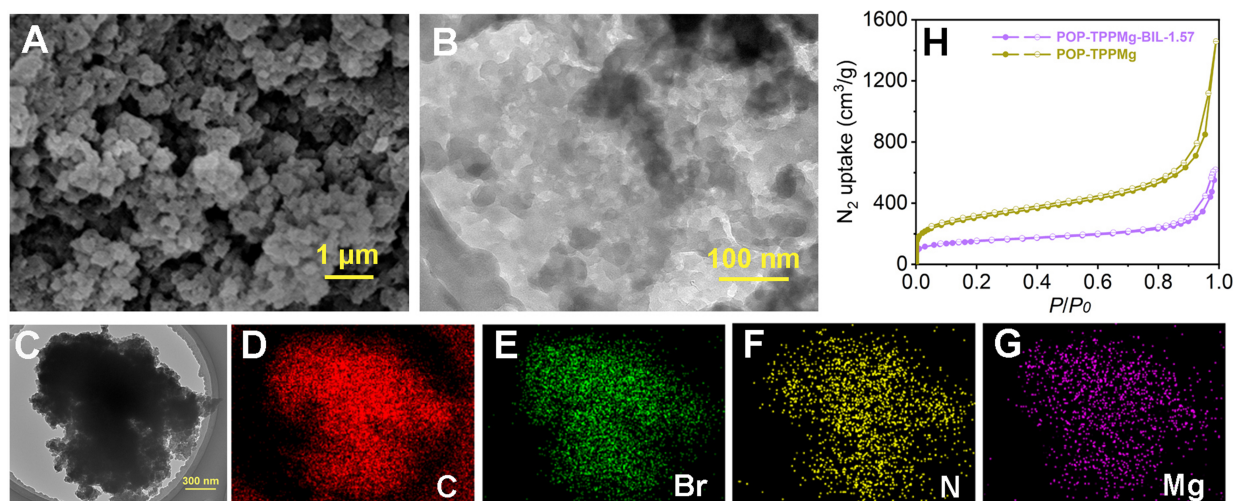


Figure 2. (A) SEM, (B) high-resolution TEM images, (C–G) large-scale TEM images, along with the corresponding elemental mapping of POP-TPPMg-BIL-1.57, and (H) N_2 sorption isotherms collected. SEM: Scanning electron microscopy; TEM: transmission electron microscopy; POP-TPPMg: polymeric Mg metalated, vinyl-functionalized tetraphenylporphyrin monomer.

composites, maintaining integrity up to 300 °C [Supplementary Figure 3]. For a comprehensive analysis, we chose POP-TPPMg-BIL-1.57 as a representative sample. To examine the morphological characteristics of these materials both before and after integration with the polymeric cross-linked ionic liquid, we utilized techniques such as SEM and TEM [Figure 2A and B, Supplementary Figure 4]. The corresponding images revealed maintained pore structures after integration with the polymeric ionic liquid, with no observable phase separation. TEM elemental mapping showcased a homogeneous dispersion of elements, including N, Br, and Mg, throughout the composite structure [Figure 2C–G]. The XPS spectrum of POP-TPPMg-BIL-1.57 before and after Ar^+ etching shows comparable Br species content (4.15% vs. 2.83%), indicating a relatively homogeneous distribution of the linear polymeric ionic liquids throughout the catalyst. The observed particle sizes were hundreds of nanometers, displaying surfaces that appeared rough and constituted aggregates of much finer particles, approximately ten nanometers in size. N_2 sorption isotherms conducted at -196 °C confirmed the high porosity of POP-TPPMg-BIL-1.57, revealing a BET surface area of 534 m^2/g and a pore volume of 0.96 cm^3/g , which is smaller compared to the pristine POP-TPPMg. The latter exhibited a BET surface area and pore volume of 1,033 m^2/g and 2.26 cm^3/g , respectively [Figure 2H].

The local chemical structure of the composite was analyzed using various spectroscopic techniques, including Fourier-transform infrared spectroscopy (FT-IR), XPS, and solid-state ^{13}C NMR spectroscopy. In the FT-IR spectrum of POP-TPPMg-BIL-1.57, the appearance of the characteristic bands of the imidazolium ring at 1,160 cm^{-1} confirmed the successful integration of ionic liquid species [Figure 3A]. This integration was further supported by the detection of a Br signal in the XPS survey of POP-TPPMg-BIL-1.57. The N 1s XPS spectrum of the composite displayed three distinct peaks at binding energies of 397.7, 399.5, and 401.7 eV [Figure 3B and Supplementary Figure 5]. These peaks were attributed to N species originating from the porphyrin ring, imidazolium component and the metal-porphyrin ring, respectively. Quantitative analysis based on the integrated areas of these N species indicated an imidazolium/Br content of 1.14 mmol/g in the composite. Moreover, the Mg content, as determined by ICP-OES, was found to be 2.09 wt%, which equates to 0.87 mmol/g. The transformation from vinyl-functionalized monomers to a highly polymerized structure was evidenced in the solid-state ^{13}C NMR spectrum. This was indicated by the absence of peaks in the 110.0 to 120.0 ppm range, which are typically associated with vinyl groups [Figure 3C]. Concurrently, the appearance of strong peaks at 28.2 and 55.3 ppm was noted, corresponding to the polymerized vinyl groups from the porphyrin and ionic liquid components, respectively. A comprehensive

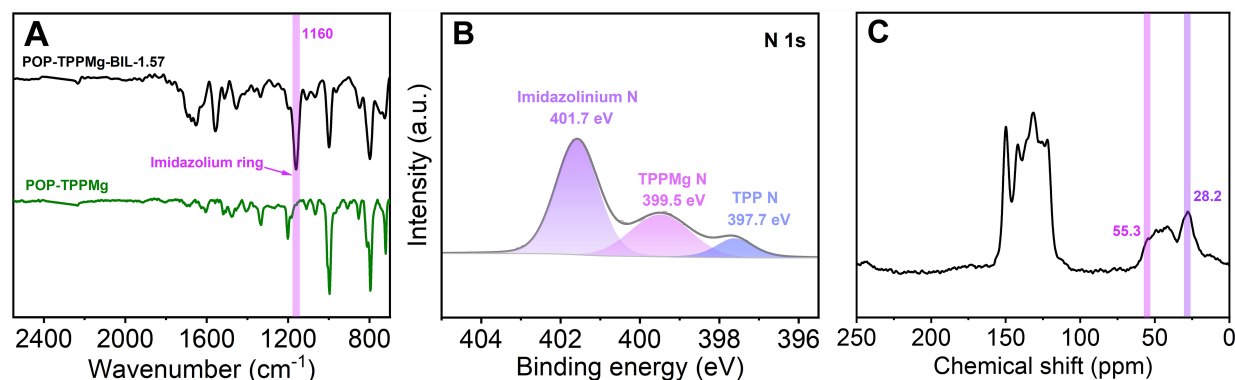


Figure 3. (A) FT-IR spectra, (B) N 1s XPS spectrum, and (C) solid-state ^{13}C NMR spectrum of POP-TPPMg-BIL-1.57. FT-IR: Fourier-transform infrared spectroscopy; XPS: X-ray photoelectron spectroscopy; NMR: nuclear magnetic resonance; POP-TPPMg: polymeric Mg metalated, vinyl-functionalized tetraphenylporphyrin monomer.

assignment of the solid-state ^{13}C NMR signals is detailed in [Supplementary Figure 6](#). The CO_2 sorption capacity of POP-TPPMg-BIL-1.57 was evaluated through sorption isotherms at temperatures of 0 and 25 $^{\circ}\text{C}$. The results showed CO_2 uptake capacities of 1.78 and 1.06 mmol/g at these temperatures, respectively. From these observations, the isosteric heat (Q_{st}) of adsorption for POP-TPPMg-BIL-1.57 was calculated to be 28.8 kJ/mol, utilizing the Virial Method [[Supplementary Figure 7](#)].

Catalytic evaluation

[Figure 4](#) showcases the catalytic efficiency of various systems in the cycloaddition of 1,2-epoxybutane and CO_2 . This data highlights the successful synergy achieved by combining dual catalytic centers in the specially designed, flexible, porous polymeric porphyrin and ionic liquid composite networks. To amplify potential differences in catalytic efficiency, we performed the reactions in the presence of a relatively low catalyst dosage (0.167 mol% and 0.262 mol% based on the amount of Mg and Br species, respectively). Notably, POP-TPPMg-BIL-1.57 exhibited an impressive catalytic conversion of 60% for 1,2-epoxybutane after 48 h at 50 $^{\circ}\text{C}$ under atmospheric CO_2 pressure, with selectivity for cyclic carbonate exceeding 99% [[Figure 4](#)]. To explore the synergistic effect of the two types of catalytic centers, we evaluated the performance of PBIL, POP-TPPMg, and their physical mixture POP-TPPMg&PBIL, under identical conditions. The results showed that the conversion for 1,2-epoxybutane was only 2%, 0%, and 11%, respectively, significantly lower than the 60% achieved by POP-BIL-TPPMg-1.57 [[Figure 4A](#)]. Moreover, a catalytic conversion of 93.0% and a selectivity of 99.0% can be achieved by increasing the catalyst loading of POP-TPPMg-BIL-1.57 to 0.333 mol%. This performance is comparable to that achieved by molecular catalysts TPPMg&BIL and the combination of heterogeneous and molecular catalysts (POP-TPPMg&BIL) [[Supplementary Table 1](#)], and superior to other catalytic systems reported in the literature for the cycloaddition of CO_2 with epoxides [[Supplementary Table 2](#)], highlighting the effective synergy between the catalytic components in POP-TPPMg-BIL-1.57. These findings underscore the efficacy of the integrated flexible framework and interweaving strategy in harnessing the synergy of different catalytic species. We also investigated how the ratio of the two types of catalytic centers within the composite influences the catalytic outcome. By varying the concentration of v-BIL during *in-situ* polymerization, we modified the ratio of v-BIL to POP-TPPMg, generating various POP-TPPMg-BIL-*x* composites (where *x* represents the molar ratio of imidazole salt to TPPMg moieties in the POP-TPPMg during synthesis, with values of 0.37, 1.57, 3.66, 8.60). This allowed us to investigate the influence of imidazole ionic liquid content on catalytic performance. Observations revealed that increasing the imidazole content from *x* = 0.37 to 1.57 resulted in a rise in the conversion of 1,2-epoxybutane from 21% to 60%. However, further escalation of the imidazole content to 3.66 and 8.60 led to a decline in the conversion rate to 54% and 37%, respectively [[Figure 4B](#)]. This trend suggests that there is

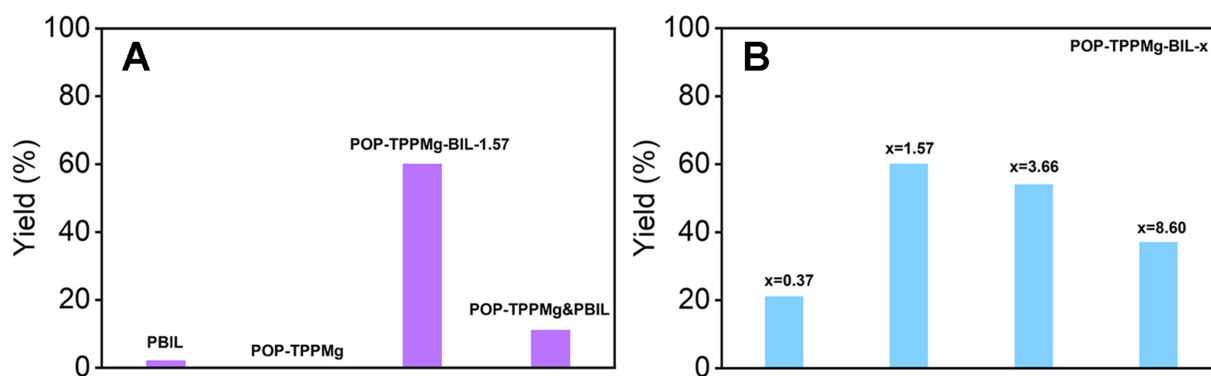


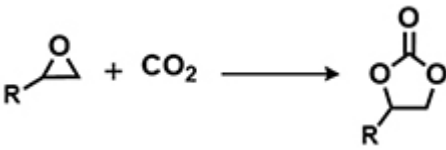

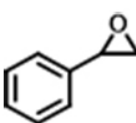
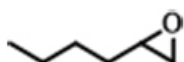
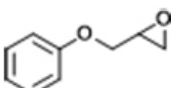
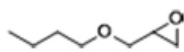
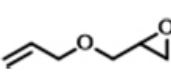
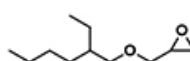

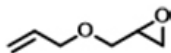
Figure 4. (A) Comparison of catalytic performance in the cycloaddition of 1,2-epoxybutane with CO₂ across diverse catalytic systems. Reaction conditions: 1,2-epoxybutane (1.08 g, 15 mmol), catalyst (0.167 mol% and 0.524 mol% based on the content of Mg and Br species, respectively, if applicable), 48 h, CO₂ (1 atm), and 50 °C; (B) Exploration of the influence of the mole ratio of the v-BIL to the TPPMg species in POP-TPPMg. The catalyst amount is adjusted according to the Mg content (0.167 mol%), and all other reaction conditions are consistent with (A). v-BIL: 3,3'-(ethane-1,2-diyl)bis(1-vinyl-1H-imidazol-3-ium); POP-TPPMg: polymeric Mg metalated, vinyl-functionalized tetraphenylporphyrin monomer.

an optimal concentration of imidazole moieties for maximizing catalytic efficiency, beyond which the performance starts to decline. This is because when the content of imidazole salt is low, part of TPPMg is not effectively utilized, while an excess of imidazole salt leads to blockage of some pores, affecting the catalytic reaction, which is also confirmed by N₂ adsorption results [Supplementary Figure 8].

Based on our experimental results and density functional theory (DFT) studies [Supplementary Figures 9 and 10], we propose a tentative reaction mechanism to explain the cooperative interaction between the metalloporphyrin and ionic components in our catalytic system. Initially, the metalloporphyrin serves as a Lewis acid center, activating the epoxide, while the ionic liquid acts as a Lewis base, supplying halide anions to promote the ring-opening of the epoxide. The calculated energy barrier for this step is 36.94 kcal/mol, significantly lower than the reported barrier of 59.0 kcal/mol for the uncatalyzed cycloaddition reaction between CO₂ and epoxides. This finding highlights the synergy between the two catalytically active sites in POP-TPPMg-BIL-1.57, which effectively reduces the energy barrier and accelerates the reaction. Subsequently, CO₂ rapidly inserts between the Lewis acid center and the oxygen anion, followed by ring closure and the release of halide ions, ultimately leading to the formation of the cycloaddition product [Supplementary Figure 11]^[57,58].

To assess the adaptability of the heterogeneous catalyst POP-TPPMg-BIL-1.57 with diverse substrates, its efficacy in CO₂ cycloaddition was evaluated using seven different epoxide substrates. The data in Table 1 and Supplementary Figure 12, entries 1-6, indicate that POP-TPPMg-BIL-1.57 successfully converted all examined substrates into their corresponding products, achieving high yields, albeit some requiring slightly higher temperatures for optimal efficiency. Furthermore, the durability of POP-TPPMg-BIL-1.57 was explored, as illustrated in Supplementary Figure 13. Over six recycling iterations, the catalyst consistently exhibited a high selectivity of 99%, with only a slight decline in activity [Table 1, entry 1]. XPS analysis was conducted to assess the composition and chemical state of the recycled POP-TPPMg-BIL-1.57 catalyst, revealing similar characteristics to the as-synthesized catalyst in terms of relative integrated areas and binding energies of Mg and Br species [Supplementary Figure 14]. Furthermore, N₂ sorption isotherm and TEM images of the reused catalyst confirmed the preservation of its pore structure [Supplementary Figures 15 and 16]. Additionally, ICP analysis of Mg species in the POP-TPPMg-BIL-1.57 catalyst before and after catalysis shows that the content of Mg species remains consistent (0.87 mmol/g vs. 0.85 mmol/g), indicating the stability of the catalyst. Therefore, we attribute the reduced productivity of the POP-TPPMg-BIL-1.57

Table 1. Cycloaddition of CO₂ with various substrates over distinct catalysts^a

<div></div>					
Entry	Substrate		T (°C)	Time (h)	Yield (%) ^b
1		POP-TPPMg-BIL-1.57	50	48	93 (88)
		POP-TPPMg-BIL-1.57 ^c	50	48	72
		POP-TPPMg-BIL-1.57	100	48	89 (84)
2		PBIL	100	48	7.2
		POP-TPPMg	100	48	< 1.0
		POP-TPPMg&PBIL	100	48	13.3
		POP-TPPMg-BIL-1.57	100	48	88 (82)
3		PBIL	100	48	6.3
		POP-TPPMg	100	48	< 1.0
		POP-TPPMg&PBIL	100	48	17.9
		POP-TPPMg-BIL-1.57	100	48	76
4		PBIL	100	48	23
		POP-TPPMg	100	48	< 1.0
		POP-TPPMg&PBIL	100	48	47.2
		POP-TPPMg-BIL-1.57	100	48	99 (92)
5		PBIL	100	48	21.6
		POP-TPPMg	100	48	< 1.0
		POP-TPPMg&PBIL	100	48	42.4
		POP-TPPMg-BIL-1.57	100	48	83
6		PBIL	100	48	32.3
		POP-TPPMg	100	48	< 1.0
		POP-TPPMg&PBIL	100	48	63.3
		POP-TPPMg-BIL-1.57	100	48	65.4
7		PBIL	100	48	< 1.0
		POP-TPPMg	100	48	< 1.0
		POP-TPPMg&PBIL	100	48	2
		POP-TPPMg-BIL-1.57	100	48	3
8		PBIL	100	48	< 1.0
		POP-TPPMg	100	48	< 1.0
		POP-TPPMg&PBIL	100	48	< 1.0
		POP-TPPMg-BIL-1.57	100	108	88 (82)
9 ^d		PBIL	100	48	31.8
		POP-TPPMg	100	48	< 1.0
		POP-TPPMg&PBIL	100	48	58.5

^aReaction conditions: epoxides (10 mmol), POP-TPPMg-BIL-1.57 catalyst (44.4 mg, 0.333 mol% and 1.046 mol% based on Mg and Br species, respectively), and CO₂ (1 atm). ^bProduct yield determined by ¹H NMR (isolated yield in parentheses). ^cAfter recycling for 6 times. ^dEpoxide (10.1 mmol), POP-TPPMg-BIL-1.57 catalyst (13 mg). POP-TPPMg: Polymeric Mg metalated, vinyl-functionalized tetraphenylporphyrin monomer; PBIL: polymeric 3,3'-(ethane-1,2-diyl)bis(1-vinyl-1H-imidazol-3-ium) bromide; NMR: nuclear magnetic resonance.

catalyst to catalyst degradation during recycling. To validate this, a larger-scale experiment was conducted with a substrate to catalyst ratio of 1,000. In this setup, POP-TPPMg-BIL-1.57 efficiently catalyzed the reaction of allyl glycidyl ether and CO₂ into the target cyclic carbonates with an approximate yield of 88% [Table 1, entry 9]. Significantly, no traces of Mg or imidazolium species were detected in the filtrate, and the reaction was completely quenched after the catalyst was hot-filtered, confirming the heterogeneous nature of the catalyst [Supplementary Figure 17].

To validate the universality of this approach, we successfully extended it to a bipyridine porous polymer derived from the radical polymerization of 5,5'-divinyl-2,2'-bipyridine, which was *in situ* integrated with a cross-linked ionic polymer (PBIL), and subsequently complexed with Cu²⁺ ions to create a Lewis acid and ionic liquid bifunctional polymer, POP-BpyCu-BIL-x [Supplementary Figures 18 and 19]. The cycloaddition reaction of CO₂ with 1,2-epoxybutane demonstrated that under conditions of 50 °C and one atmosphere, POP-BpyCu-BIL-0.86 exhibited excellent catalytic performance, achieving a catalytic conversion of 70.4% over 48 h [Supplementary Table 3, entry 1]. Although this activity is lower than that of the corresponding homogeneous catalytic system [Supplementary Table 3, entries 2 and 3], it significantly surpasses the physically mixed binary catalytic system POP-BpyCu&PBIL, which achieved a yield of only 44.8% [Supplementary Table 3, entry 4]. This indicates effective cooperation between the two distinct catalytic centers in POP-BpyCu-BIL-0.86. This conclusion is further supported by POP-BpyCu-BIL-0.14, which, having a lower ionic liquid content and similar copper content as POP-BpyCu-BIL-0.86, exhibited lower catalytic activity with a yield of 43.5% under the same conditions [Supplementary Table 3, entry 5].

CONCLUSIONS

In summary, our research has resulted in the development of composites featuring two distinct catalytically active species, each embedded within a flexible framework. These centers have demonstrated synergistic effects, significantly enhancing catalytic performance in the cycloaddition of CO₂ and epoxides, showcasing notable improvements in both activity and selectivity. Subsequent examinations of these bifunctional heterogeneous catalysts revealed their facile separability and reusability, maintaining efficacy and stability across multiple cycles. Inspired by the diverse applications of polymers derived from vinyl polymerization, this methodology introduces a novel approach to designing catalytic systems with multiple, cooperatively functioning catalytic centers. This work represents a significant breakthrough in catalyst design, presenting an innovative strategy for the development of bifunctional catalysts endowed with dual activation capabilities.

DECLARATIONS

Acknowledgments

We appreciate the assistance of Fang Chen from Analytical Testing Center of the Department of Chemistry, Zhejiang University, in conducting SEM and TEM measurements.

Authors' contributions

Designed the experiments, carried out characterization, analyzed data, interpreted results, and drew the pictures: Zheng, L.

Synthesized samples: Fang, C.; Han, J.

Conducted material characterization: Wang, Z.; Dai, T.; Chen, Z.; Ma, J.

Directed and supervised the project, analyzed data, and wrote and revised the manuscript: Dai, Z.; Xiong, Y.; Sun, Q.

Availability of data and materials

The data substantiating the findings presented in this manuscript are available in the [Supplementary Materials](#) or can be obtained by contacting the corresponding authors upon reasonable request.

Financial support and sponsorship

This work was supported by the National Natural Science Foundation of China (21774101, 21902145, and 22072132), the Natural Science Foundation of Zhejiang Province (LY22B030006), and the Fundamental Research Funds of Zhejiang Sci-Tech University (22062308-Y).

Conflicts of interest

Chen, Z. is affiliated with Kente catalysts Inc., Modern Industrial Cluster. The other authors declared that there are no conflicts of interest.

Ethical approval and consent to participate

Not applicable.

Consent for publication

Not applicable.

Copyright

© The Author(s) 2026.

Supplementary Materials

[Supplementary Materials](#)

REFERENCES

1. Gao, W.; Liang, S.; Wang, R.; et al. Industrial carbon dioxide capture and utilization: state of the art and future challenges. *Chem. Soc. Rev.* **2020**, *49*, 8584–686. [DOI](#)
2. Breyer, C.; Fasihi, M.; Bajamundi, C.; Creutzig, F. Direct air capture of CO₂: a key technology for ambitious climate change mitigation. *Joule* **2019**, *3*, 2053–7. [DOI](#)
3. Alcalde, J.; Flude, S.; Wilkinson, M.; et al. Estimating geological CO₂ storage security to deliver on climate mitigation. *Nat. Commun.* **2018**, *9*, 2201. [DOI PubMed PMC](#)
4. Davis, S. J.; Caldeira, K.; Matthews, H. D. Future CO₂ emissions and climate change from existing energy infrastructure. *Science* **2010**, *329*, 1330–3. [DOI PubMed](#)
5. Wang, W.; Wang, S.; Ma, X.; Gong, J. Recent advances in catalytic hydrogenation of carbon dioxide. *Chem. Soc. Rev.* **2011**, *40*, 3703–27. [DOI](#)
6. Xu, X.; Wei, Q.; Xi, Z.; et al. Research progress of metal-organic frameworks-based materials for CO₂ capture and CO₂-to-alcohols conversion. *Coord. Chem. Rev.* **2023**, *495*, 215393. [DOI](#)
7. Song, K. S.; Fritz, P. W.; Coskun, A. Porous organic polymers for CO₂ capture, separation and conversion. *Chem. Soc. Rev.* **2022**, *51*, 9831–52. [DOI PubMed PMC](#)
8. Kumar, A.; Bhardwaj, R.; Choudhury, J. Integrated CO₂ capture and conversion to methanol leveraged by the transfer hydrogenation approach. *ACS. Catal.* **2023**, *13*, 927–33. [DOI](#)
9. Siegel, R. E.; Pattanayak, S.; Berben, L. A. Reactive capture of CO₂: opportunities and challenges. *ACS. Catal.* **2023**, *13*, 766–84. [DOI](#)
10. Medinger, J.; Song, K. S.; Umubyeyi, P.; Coskun, A.; Lattuada, M. Magnetically guided synthesis of anisotropic porous carbons toward efficient CO₂ capture and magnetic separation of oil. *ACS. Appl. Mater. Interfaces.* **2023**, *15*, 21394–402. [DOI PubMed](#)
11. Wan, M.; Yang, Z.; Morgan, H.; et al. Enhanced CO₂ reactive capture and conversion using aminothiolate ligand-metal interface. *J. Am. Chem. Soc.* **2023**, *145*, 26038–51. [DOI](#)
12. Zhang, B.; Shi, J.; Chu, Z.; et al. Lysine-modulated synthesis of enzyme-embedded hydrogen-bonded organic frameworks for efficient carbon dioxide fixation. *Chem. Synth.* **2023**, *3*, 5. [DOI](#)
13. Dongare, S.; Coskun, O. K.; Cagli, E.; et al. A bifunctional ionic liquid for capture and electrochemical conversion of CO₂ to CO over silver. *ACS. Catal.* **2023**, *13*, 7812–21. [DOI PubMed PMC](#)
14. Yin, Y.; Kang, X.; Han, B. Two-dimensional materials: synthesis and applications in the electro-reduction of carbon dioxide. *Chem. Synth.* **2022**, *2*, 19. [DOI](#)
15. Kar, S.; Goeppert, A.; Galvan, V.; Chowdhury, R.; Olah, J.; Prakash, G. K. S. A carbon-neutral CO₂ capture, conversion, and utilization cycle with low-temperature regeneration of sodium hydroxide. *J. Am. Chem. Soc.* **2018**, *140*, 16873–6. [DOI PubMed](#)
16. Di, J.; Hao, G.; Liu, G.; Zhou, J.; Jiang, W.; Liu, Z. Defective materials for CO₂ photoreduction: from C₁ to C₂₊ products. *Coord. Chem. Rev.* **2023**, *482*, 215057. [DOI](#)

17. Zhang, Z.; Yang, Z.; Liu, L.; Wang, Y.; Kawi, S. Catalytic CO₂ conversion to C1 chemicals over single-atom catalysts. *Adv. Energy Mater.* **2023**, *13*, 2301852. DOI
18. Trogadas, P.; Xu, L.; Coppens, M. O. From biomimicking to bioinspired design of electrocatalysts for CO₂ reduction to C₁ products. *Angew. Chem. Int. Ed. Engl.* **2024**, *63*, e202314446. DOI PubMed PMC
19. Yang, Z.; Chen, H.; Li, B.; et al. Topotactic synthesis of phosphabenzene-functionalized porous organic polymers: efficient ligands in CO₂ conversion. *Angew. Chem. Int. Ed. Engl.* **2019**, *58*, 13763-7. DOI
20. Luo, R.; Chen, Y.; He, Q.; et al. Metallosalen-based ionic porous polymers as bifunctional catalysts for the conversion of CO₂ into valuable chemicals. *ChemSusChem* **2017**, *10*, 1526-33. DOI
21. Zhong, H.; Su, Y.; Chen, X.; Li, X.; Wang, R. Imidazolium- and triazine-based porous organic polymers for heterogeneous catalytic conversion of CO₂ into cyclic carbonates. *ChemSusChem* **2017**, *10*, 4855-63. DOI
22. Luo, R.; Chen, M.; Zhou, F.; et al. Synthesis of metalloporphyrin-based porous organic polymers and their functionalization for conversion of CO₂ into cyclic carbonates: recent advances, opportunities and challenges. *J. Mater. Chem. A* **2021**, *9*, 25731-49. DOI
23. Dai, Z.; Tang, Y.; Zhang, F.; et al. Combination of binary active sites into heterogeneous porous polymer catalysts for efficient transformation of CO₂ under mild conditions. *Chin. J. Catal.* **2021**, *42*, 618-26. DOI
24. Wan, Y. L.; Zhang, J.; Wang, L.; Lei, Y. Z.; Wen, L. L. Poly(ionic liquid)-coated hydroxy-functionalized carbon nanotube nanoarchitectures with boosted catalytic performance for carbon dioxide cycloaddition. *J. Colloid. Interface. Sci.* **2024**, *653*, 844-56. DOI
25. Zhao, Y.; Zhu, S.; Liao, C.; et al. Cobalt-mediated switchable catalysis for the one-pot synthesis of cyclic polymers. *Angew. Chem. Int. Ed. Engl.* **2021**, *60*, 16974-9. DOI
26. Liu, F.; Huang, K.; Wu, Q.; Dai, S. Solvent-free self-assembly to the synthesis of nitrogen-doped ordered mesoporous polymers for highly selective capture and conversion of CO₂. *Adv. Mater.* **2017**, *29*, 1700445. DOI
27. Luo, R.; Yang, Y.; Chen, K.; et al. Tailored covalent organic frameworks for simultaneously capturing and converting CO₂ into cyclic carbonates. *J. Mater. Chem. A* **2021**, *9*, 20941-56. DOI
28. Huang, K.; Zhang, J.; Liu, F.; Dai, S. Synthesis of porous polymeric catalysts for the conversion of carbon dioxide. *ACS. Catal.* **2018**, *8*, 9079-102. DOI
29. Liang, J.; Huang, Y.; Cao, R. Metal-organic frameworks and porous organic polymers for sustainable fixation of carbon dioxide into cyclic carbonates. *Coord. Chem. Rev.* **2019**, *378*, 32-65. DOI
30. Han, W.; Ma, X.; Wang, J.; Leng, F.; Xie, C.; Jiang, H. L. Endowing porphyrinic metal-organic frameworks with high stability by a linker desymmetrization strategy. *J. Am. Chem. Soc.* **2023**, *145*, 9665-71. DOI PubMed
31. Su, Y.; Yuan, G.; Hu, J.; et al. Recent progress in strategies for preparation of metal-organic frameworks and their hybrids with different dimensions. *Chem. Synth.* **2022**, *3*, 1. DOI
32. Li, H.; Li, C.; Wang, Y.; et al. Selenium confined in ZIF-8 derived porous carbon@MWCNTs 3D networks: tailoring reaction kinetics for high performance lithium-selenium batteries. *Chem. Synth.* **2022**, *2*, 8. DOI
33. Liu, L.; Wang, S. M.; Han, Z. B.; Ding, M.; Yuan, D. Q.; Jiang, H. L. Exceptionally robust in-based metal-organic framework for highly efficient carbon dioxide capture and conversion. *Inorg. Chem.* **2016**, *55*, 3558-65. DOI
34. Feng, D.; Chung, W. C.; Wei, Z.; et al. Construction of ultrastable porphyrin Zr metal-organic frameworks through linker elimination. *J. Am. Chem. Soc.* **2013**, *135*, 17105-10. DOI
35. Song, J.; Zhang, Z.; Hu, S.; Wu, T.; Jiang, T.; Han, B. MOF-5/*n*-Bu₄NBr: an efficient catalyst system for the synthesis of cyclic carbonates from epoxides and CO₂ under mild conditions. *Green. Chem.* **2009**, *11*, 1031. DOI
36. Dai, Z.; Sun, Q.; Liu, X.; et al. Metalated porous porphyrin polymers as efficient heterogeneous catalysts for cycloaddition of epoxides with CO₂ under ambient conditions. *J. Catal.* **2016**, *338*, 202-9. DOI
37. Xie, Y.; Wang, T. T.; Liu, X. H.; Zou, K.; Deng, W. Q. Capture and conversion of CO₂ at ambient conditions by a conjugated microporous polymer. *Nat. Commun.* **2013**, *4*, 1960. DOI PubMed PMC
38. Xie, Y.; Wang, T. T.; Yang, R. X.; Huang, N. Y.; Zou, K.; Deng, W. Q. Efficient fixation of CO₂ by a zinc-coordinated conjugated microporous polymer. *ChemSusChem* **2014**, *7*, 2110-4. DOI PubMed
39. Gao, W. Y.; Chen, Y.; Niu, Y.; et al. Crystal engineering of an nbo topology metal-organic framework for chemical fixation of CO₂ under ambient conditions. *Angew. Chem. Int. Ed. Engl.* **2014**, *53*, 2615-9. DOI
40. Zhi, Y.; Shao, P.; Feng, X.; et al. Covalent organic frameworks: efficient, metal-free, heterogeneous organocatalysts for chemical fixation of CO₂ under mild conditions. *J. Mater. Chem. A* **2018**, *6*, 374-82. DOI
41. Li, H.; Feng, X.; Shao, P.; et al. Synthesis of covalent organic frameworks *via in situ* salen skeleton formation for catalytic applications. *J. Mater. Chem. A* **2019**, *7*, 5482-92. DOI

42. Zhou, W.; Deng, Q. W.; Ren, G. Q.; et al. Enhanced carbon dioxide conversion at ambient conditions via a pore enrichment effect. *Nat. Commun.* **2020**, *11*, 4481. DOI PubMed PMC
43. Sengupta, M.; Bag, A.; Ghosh, S.; Mondal, P.; Bordoloi, A.; Islam, S. M. Cu₂O₃@COF: an efficient heterogeneous catalyst system for CO₂ cycloadditions under ambient conditions. *J. CO₂ Util.* **2019**, *34*, 533–42. DOI
44. Sun, Q.; Aguila, B.; Perman, J.; Nguyen, N.; Ma, S. Flexibility matters: cooperative active sites in covalent organic framework and threaded ionic polymer. *J. Am. Chem. Soc.* **2016**, *138*, 15790–6. DOI PubMed
45. Aguila, B.; Sun, Q.; Wang, X.; et al. Lower activation energy for catalytic reactions through host-guest cooperation within metal-organic frameworks. *Angew. Chem. Int. Ed. Engl.* **2018**, *57*, 10107–11. DOI
46. Ding, M.; Jiang, H. Incorporation of imidazolium-based poly(ionic liquid)s into a metal–organic framework for CO₂ capture and conversion. *ACS. Catal.* **2018**, *8*, 3194–201. DOI
47. Sun, Q.; Ma, S.; Dai, Z.; Meng, X.; Xiao, F. A hierarchical porous ionic organic polymer as a new platform for heterogeneous phase transfer catalysis. *J. Mater. Chem. A.* **2015**, *3*, 23871–5. DOI
48. Sun, Q.; Aguila, B.; Verma, G.; et al. Superhydrophobicity: constructing homogeneous catalysts into superhydrophobic porous frameworks to protect them from hydrolytic degradation. *Chem* **2016**, *1*, 628–39. DOI
49. Dai, Z.; Bao, Y.; Yuan, J.; Yao, J.; Xiong, Y. Different functional groups modified porous organic polymers used for low concentration CO₂ fixation. *Chem. Commun.* **2021**, *57*, 9732–5. DOI
50. Sun, Q.; Xiao, F. Porous polymeric catalysts constructed from vinylated functionalities. *Acc. Mater. Res.* **2022**, *3*, 772–81. DOI
51. Wang, X.; Dong, Q.; Xu, Z.; et al. Hierarchically nanoporous copolymer with built-in carbene-CO₂ adducts as halogen-free heterogeneous organocatalyst towards cycloaddition of carbon dioxide into carbonates. *Chem. Eng. J.* **2021**, *403*, 126460. DOI
52. Duval, A.; Avérous, L. Solvent- and halogen-free modification of biobased polyphenols to introduce vinyl groups: versatile aromatic building blocks for polymer synthesis. *ChemSusChem* **2017**, *10*, 1813–22. DOI PubMed
53. Zhou, S.; Luo, X.; Zhang, Y.; et al. Post-cationic modification of a porphyrin-based conjugated microporous polymer for enhanced removal performance of bisphenol A. *Chem. Commun.* **2023**, *59*, 14399–402. DOI
54. Zhang, P.; Wang, S.; Ma, S.; Xiao, F. S.; Sun, Q. Exploration of advanced porous organic polymers as a platform for biomimetic catalysis and molecular recognition. *Chem. Commun.* **2020**, *56*, 10631–41. DOI
55. Sun, Q.; Song, Y.; Aguila, B.; Ivanov, A. S.; Bryantsev, V. S.; Ma, S. Spatial engineering direct cooperativity between binding sites for uranium sequestration. *Adv. Sci.* **2021**, *8*, 2001573. DOI PubMed PMC
56. Dai, Z.; Sun, Q.; Liu, X.; et al. A hierarchical bipyridine-constructed framework for highly efficient carbon dioxide capture and catalytic conversion. *ChemSusChem* **2017**, *10*, 1186–92. DOI
57. Li, X.; Niu, X.; Fu, P.; et al. Macrocyclic-on-COF photocatalyst constructed by in-situ linker exchange for efficient photocatalytic CO₂ cycloaddition. *Appl. Catal. B. Environ. Energy.* **2024**, *350*, 123943. DOI
58. Ma, D.; Song, Y.; Zhao, H.; et al. Ordered macro–microporous covalent organic frameworks as bifunctional catalysts for CO₂ cycloaddition. *ACS. Sustain. Chem. Eng.* **2023**, *11*, 6183–90. DOI

Disclaimer/Publisher’s Note: All statements, opinions, and data contained in this publication are solely those of the individual author(s) and contributor(s) and do not necessarily reflect those of OAE and/or the editor(s). OAE and/or the editor(s) disclaim any responsibility for harm to persons or property resulting from the use of any ideas, methods, instructions, or products mentioned in the content.



© The Author(s) 2026. Open Access This article is licensed under a Creative Commons Attribution 4.0 International License (<https://creativecommons.org/licenses/by/4.0/>), which permits unrestricted use, sharing, adaptation, distribution and reproduction in any medium or format, for any purpose, even commercially, as long as you give appropriate credit to the original author(s) and the source, provide a link to the Creative Commons license, and indicate if changes were made.

**Liping Zheng**

Liping Zheng earned his master's degree from Zhejiang Sci-Tech University under the supervision of Dr. Zhifeng Dai. His research focuses on the development and application of porous organic polymer catalysts.

**Can Fang**

Can Fang is currently pursuing a master's degree at Zhejiang Sci-Tech University under the supervision of Dr. Zhifeng Dai. Her research centers on the development of novel porous organic polymers for CO₂ transformation.

**Zhenghai Chen**

Zhenghai Chen graduated from Zhejiang University in 1989 and is currently serving as the Director and Executive Deputy General Manager at Kentte Catalysts Inc. He specializes in phase transfer catalysts, quaternary ammonium bases, and high-purity electrolytes.

**Jinxu Han**

Jinxu Han is currently a master's student at Zhejiang Sci-Tech University under the supervision of Dr. Zhifeng Dai. His research focuses on the design and construction of porous organic polymer membranes for catalysis.

**Zhouxian Wang**

Zhouxian Wang is a master's student at Zhejiang Sci-Tech University under the supervision of Dr. Zhifeng Dai. His research focuses on developing porous organic polymers for the adsorption and separation of SO_2 .

**Tonghao Dai**

Tonghao Dai is an undergraduate student at the School of Chemistry and Chemical Engineering, Zhejiang Sci-Tech University, under the mentorship of Dr. Zhifeng Dai. His research focuses on the development of porous organic polymers for the adsorption and separation of NH_3 .

**Jiacong Ma**

Jiacong Ma is a master's student at Zhejiang Sci-Tech University under the supervision of Dr. Zhifeng Dai, with research focused on the construction of porous organic polymers.

**Zhifeng Dai**

Zhifeng Dai obtained his Ph.D. from Zhejiang University in 2017. Since November 2018, he has served as a lecturer and associate professor at Zhejiang Sci-Tech University. His research interests include the development of functional organic polymer materials and their applications.

**Yubing Xiong**

Yubing Xiong is a professor at Zhejiang Sci-Tech University and the director of the Key Laboratory of Polymer Materials Surface and Interface Science in Zhejiang Province. His research focuses on functional polymer materials based on ionic liquids and CO₂ conversion.

**Qi Sun**

Qi Sun earned her Ph.D. from Zhejiang University in 2014 and subsequently undertook postdoctoral research at the University of South Florida. In September 2019, she joined the College of Chemical and Biological Engineering at Zhejiang University as a “Hundred Talent” tenure-track professor. Her current research focuses on developing covalent organic framework membranes for ion separation, catalysis, and environmental remediation.